

exhibit several oxidation states, depending on the oxygen partial pressure) in which edge dislocations where observed after electron irradiation [15].

Though the use of Vegard's law can be a valuable empirical tool for engineering nuclear materials, the structural features observed in uranium oxides where a complex reorganization of the oxygen sub-lattice and significant enthalpy effects are observed do not support the hypotheses of this description. These structural reorganizations are not always well documented because accurate information on the structural parameters describing the oxygen sub-lattice requires neutron diffraction experiments. EXAFS experiments can also provide valuable information on the local environments but only few experiments were performed on $(\text{U},\text{La})\text{O}_2$ compounds.

Therefore, new experiments should be planned to achieve a better understanding of $(\text{U},\text{La})\text{O}_2$ compounds, more specifically to understand whether a significant defect clustering also occurs in these systems. Such a behavior is expected to have significant impact for the design of radiation resistant fuels consisting of mixed oxides.

REFERENCES

1. H.G. Riella, M. Durazzo, M. Hirata, R.A. Nogueira, J. Nucl. Mater. **178**, 204 (1991).
2. M.P. Herrero, R.M. Rojas, J. Solid State Chem., **73**, 536-543 (1983).
3. H. Weitzel and C. Keller, J. Solid State Chem., **13**, 136-141 (1975).
4. K. Kapoor, S.V. Ramana Rao, Sheela, T. Sanyal, A. Singh, J. Nucl. Mat. **321**, 331-334 (2003).
5. M. Kato and K. Konishi, J. Nucl. Mat. (2009) doi:10.1016/j.jnucmat.2008.09.037.
6. P. Ruello & al., J. Am. Ceram. Soc. **88**, 604 (2005).
7. P. Ruello, L. Desgranges, G. Baldinozzi, G. Calvarin, T. Hansen, G. Petot-Erras, C. Petot, Journal of Phys. Chem. Solids **66**, 823-831 (2005).
8. R.D. Shannon, Acta Cryst. A³², 751 (1976).
9. M.T. Hutchings, J. Chem. Soc., Faraday Trans. 2, **83**, 1083-1103 (1987).
10. D.J.M. Bevan, I.E. Grey, B.T.M. Willis, J. Solid State Chem. **61**, 1-7 (1986).
11. G. Baldinozzi, G. Rousseau, L. Desgranges, J.C. Nièpée, J.F. Béar, Mat. Res. Soc. Symp. Proceedings **802**, 3-8 (2003).
12. R.I. Cooper and B.T.M. Willis, Acta Cryst. A **60**, 322-325 (2004).
13. G.C. Allen and N.R. Holmes, J. Nucl. Mater. **223**, 231 (1995).
14. B.G. Hyde, Acta Cryst. A **27**, 617-621 (1971).
15. K. Yasunaga et al., Nucl. Instr. and Meth. in Phys. Res. B **266**, 2877-2881 (2008).

INTRODUCTION

Nuclear fuels based on ThO_2 are reaching great importance in the Pu inventories reduction [1] as well as in minor actinides and long life fission products diminution [2] too. The development of this new generation of nuclear fuels requires their characterization before and after irradiation. ThO_2 has been chosen like an Inert Matrix Fuel (IMF), where the carrier of the plutonium is not uranium and it should be more or less transparent to neutrons [3], due to different reasons like: the Th abundance, around three times higher than U, its melt temperature (3300 °C) and its thermal conductivity higher for ThO_2 than UO_2 , its high chemical stability (ThO_2 solubility is a thousand times less than UO_2 [4]), its better stability in the presence of radiation damage, and its higher actinide burnup. One option for this IMF after nuclear fuel cycle could be the Deep Geological Disposal and, for that purpose, it is essential to assess some criteria as its compatibility with the repository environment, chemical stability with time in the presence of known radiation fields [5].

The evaluation of Pu chemical behavior should be done hereby models with speciation

Cerium Dioxide Surface Characterization and Determination of Surface Site Density by Potentiometric Fast Titration

N. Rodriguez Villagra¹, J.C. Marugan¹, E. Iglesias¹, J. Nieto¹, T. Missana¹, N. Albaran¹, J. Cobos², J. Quiñones¹

¹Ciemat, Avda. Complutense 22, 28040 – Madrid. SPAIN

²ITU-IRC European Commission Joint Research Centre Institute for TransU Elements. European Commission, Karlsruhe, Germany

ABSTRACT

Cerium dioxide has been used as a Pu analogous to study Pu-Th mixed oxide fuels behavior. $(\text{Th}, \text{Pu})\text{O}_2$, known as "Th-MOX". They are considered as possible advanced nuclear fuels for Generation-IV Fast Reactors aiming the burning and reprocessing of Pu stocks generated on U cycle. The use of Pu in Mixed-Oxide Fuel (MOX) will generate less fission products than U dioxide fuels. Before performing the study of Th sorption behavior, it is necessary to identify essential parameters as surface coordination sites density, surface charge and the equilibrium constants of the functional surface groups of hydrous oxide. Ce oxide has been characterized by the BET (Brunauer-Emmett-Teller) method to measure the specific surface area using $\text{Na}(\text{g})$, by XRD (X-Ray Diffraction) to verify the crystalline structure, by SEM (Scanning Electron Microscopy) to analyze how well the pellets have been sintered, by AFM (Atomic Force Microscopy) to study the roughness, and by potentiometric titration to determine the surface sites density.

Potentiometric titrations were carried out both on a suspension of ceria colloids and on pellets. After the measurements, both proton intrinsic affinity constants and OH surface groups were compared. The experiments were developed in a wide range of pH and at different ionic strengths. The sites density values measured for ceria in 0.1M NaClO_4 media were 52.0 ± 5.5 and 2.3 ± 0.1 sites nm^{-2} , for colloids and pellet, respectively. The hysteresis cycle obtained with pellets between acid/alkaline directions is rather important because indicates the tendency to retain other elements in this matrix.

data. Choppin [6] proposed Th(IV) as a Pu(IV) surrogate although Th(IV) has a weaker complexation and hydrolysis than Pu(IV). Th(IV) complexation constants can be adjusted multiplying $\log [\beta(\text{Th}^{\text{IV}})]$ by Th(IV) and Pu(IV) ionic radium ratio. But this approach should be considered as a rude approximation only valid to 1:1 complexation ($\log K^{\text{a}}\text{S}^{\text{a}}\text{Th}(\text{OH})_4(\text{cr}) = -9.4$ [7]). As happened with nuclear fuels based on Th, it is assumed that radionuclide release from the matrix during the deep geological repository in Th-MOX will be controlled by the solubility of PuO_2 and $(\text{Pu}-\text{Th})\text{O}_2$ fabrication sol-gel, from a liquid "sol" (colloidal) into a solid "gel" phase and characterization (lixiviation, chemical stability,...) are being performed. Thanks to the ITU-CIEMAT framework collaboration project, characterization and Th sorption experiments on CeO_2 have been performed to be compared with Pu results. The CIEMAT major goal was to get confidence on sorption processes (including sites density determination), and finally to be able to reproduce the Th sorption mechanism in natural waters. Pu is simulated with Ce and experiments were carried out using CeO_2 pellets.

The knowledge of radionuclide sorption mechanism in underground water conditions and behavior prediction model of retention are key issues in assessing the performance of a given nuclear waste disposal concept. An essential parameter for adsorption is the surface sites density that can be measured by acid-alkaline potentiometric surface titrations. Proton exchange sites density determination consists of two steps: first, the proton adsorption in acid media, and next, the proton desorption in alkaline media. Only one type of $\equiv\text{S}-\text{OH}$ sites has been considered because there is not knowledge about CeO_2 surface behavior [8]. In the present work, we attempt to quantify the sorption behavior of Th using CeO_2 pellets together with ITU focusing on the assessment of the long term safety of Th-based fuels. It is known that Th has a great tendency to adsorb colloidal particles and oxides on its surface; this affecting the migration of Th in natural groundwater [4, 9]. In this case, Th represents the main element of spent nuclear fuel by mass. Therefore, a continuous sorption test was carried out involving Th(IV) over $\text{Ce}(\text{IV})$ dioxide (as non irradiated chemical surrogate for Pu(IV)). The main objectives of the present work are (1) to compare the surface properties of colloidal and compacted CeO_2 and (2) to study Th adsorption on compacted CeO_2 .

EXPERIMENTAL DETAILS

CeO_2 pellets were prepared by the sol-gel process in ITU. The specific surface area (BET method using both N_2 and Kr adsorbate) was measured with the ASAP 2020 equipment from Micromeritics. The values obtained were $84.74 \pm 1.82 \text{ m}^2/\text{g}$ and $0.22 \pm 0.01 \text{ m}^2/\text{g}$, respectively [10]. AFM showed the roughness depth (Figure 1).

The crystalline structure was checked by XRD using an X-Pert-MPD Philips diffractometer. The XRD pattern (Figure 2) is perfectly fit by the theoretical one, showing a cubic system with fluorite type structure, and the experimental value of the unit cell parameter ($5.411 \pm 0.012 \text{ \AA}$) is almost the same as the theoretical value (5.412 \AA).

SEM revealed surface morphology by using a FEG-SEM (Field-Emission gun Scanning Electron Microscope) at 10 kV in a JEOL 6335 equipment (Figure 3, Figure 4 and Figure 5). At low magnification (Figure 3, first image), it is possible to appreciate a rough surface. At higher magnification, it is interesting to observe a possible grain boundary and marks with a width less than $0.1 \mu\text{m}$.

Methods
The continuous fast titrations were performed under anoxic conditions inside glove box under argon atmosphere ($<1\text{ ppm O}_2$) in order to avoid CO_2 presence; the background electrolyte was 0.1 M NaClO_4 at 298 K , and the pH has been adjusted by adding precise aliquots of HCl (acidic direction $\text{pH} \approx 1.5$) or NaOH (alkaline direction until $\text{pH} \approx 12.5$), both 0.1 M . This was done under stirring (electrolytic media 0.1 M NaClO_4), ceria colloids (1 g/l) in 0.1 M NaClO_4 (40 ml) and CeO_2 pellet in 0.1 M NaClO_4 (40 ml). Equilibration time for each solution before titration was 24 hours. The titration was carried out with a 808 Titrand equipment (Metrohm). The working conditions for each measurement were saved in a method ΔE (mV) <0.5 in 5 min as maximum time. Between measurements, a delay of 60 seconds for manual adding of the aliquot was set.

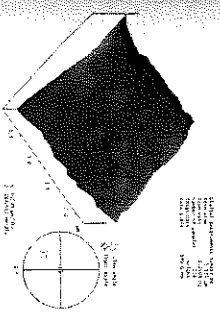


Figure 1 CeO_2 AFM surface image (scan size $2.75 \mu\text{m}$).

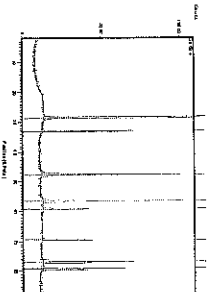


Figure 2 Characterization of CeO_2 pellet by X-ray diffraction pattern with a good agreement between experimental and theoretical results.

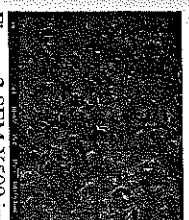


Figure 3 SEM X500 image
 CeO_2 pellet.



Figure 4 SEM X2000 image
 CeO_2 pellet.

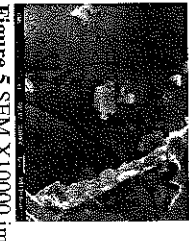


Figure 5 SEM X1000 image
 CeO_2 pellet.

The selected pH region for dynamic sequential sorption experiments was 1.5-4.5 to avoid Th hydroxides formation, because this detail complicates the Th behavior modelling. Östhols [7] predicts those alkaline or neutral pH are enough for inducing Th desorption by hydrolysis on silica surface. As the added acid or base volume and taken samples was small opposite to the initial volume (330 ml), changes in the radionuclide concentration and solid area to liquid volume ratios (S:L) could be ignored. The S_{geom}/V_s initial value was 0.25 m^{-1} .

Firstly, a pellet was washed with MilliQ water until getting neutral pH. Th⁴⁺ solution $6.01 \cdot 10^{-5} \text{ M}$ was prepared starting with 4.4 mg of ThO₂ in 49.7 ml suprapure HNO₃, 0.3 ml HClO₄ (70%, $\rho = 1.67 \cdot 10^3 \text{ kg/m}^3$ or 11.643 M) and 50 ml of 0.1M HClO₄ to get a final volume of 100 ml, electrolytic media 0.1 M NaClO₄ was added and adjusted around pH 1.5 with 0.1 M HCl under stirring. After equilibrium was reached, a CeO₂ pellet was added and one sample (1 ml filtrated with 0.22 μm filters and 1 ml ultrafiltrated under ultracentrifugation) was taken to analyze by ICP-MS. This process was followed after one day of stabilization, after modify pH with 0.1M HCl or 0.1M NaOH. A new method was created, in this case ΔE (mV) < 0.1 between 60 and 150 s.

RESULTS AND DISCUSSION

SEM of the CeO₂ pellet performed before the experiments (Figures 3- 5) showed no surface cracks and a non homogeneous porosity distribution. Potentiometric titration curves of colloids and pellet are shown in Figure 6 and Figure 7. Regarding to the acid/alkaline reversibility, a large hysteresis between the two directions is not observed. It was noted that the equilibrium in alkaline direction was reached more quickly than in the acid direction within the systematic equilibrium time used (approximately 2 minutes).

No consumption or release of protons takes place at lower pH, but above pH=4, the titration shows proton release. Additional with different ionic strengths are needed to adequately model the acid-base behavior and to calculate the active sites density.

The parameters calculated from CeO₂ are presented in Table 1. For the pellet, we have obtained $(31.90 \pm 0.93) \cdot 10^{-2} \text{ mol} \cdot \text{kg}^{-1}$. Ceria pellets carry pH-dependent negative charge as it is shown in Figure 6 and Figure 7 as a consequence of the surface charge dependency on the pH, although it will be necessary to make other tests with other ionic strengths. In Figure 8 a swift decrease in Th concentration when pH increases is shown. There are two possible reasons: Th hydroxide formation could be take place (Figure 9) or, more reasonable, Th sorption on ceria coordination sites dominates through an exchange by protons in the equilibrium time (1-3 days). Otherwise, the difference in Th concentration between filtered and ultrafiltered samples decreases as the pH increases, which indicates that at the beginning of the experiment there was Th in colloidal form. In future works, it would be necessary to develop experiments on Th sorption for constant pH, thus it would be possible to establish K_d on the basis of those conditions.

As expected, the Ce concentration levels in solution remain relatively constant since the beginning; it means that in the test conditions there have been no dissolution of Ce.

Table I. Summary of the values calculated on Ce dioxide colloids and pellet.

	Colloids	Pellet
$a / \text{kg} \cdot \text{l}^{-1}$	$(1.00 \pm 0.02) \cdot 10^{-3}$	$(55.9 \pm 1.4) \cdot 10^{-4}$
C_A / M	$(205.72 \pm 0.14) \cdot 10^{-4}$	$(153.26 \pm 0.15) \cdot 10^{-4}$
$[\text{H}^+]_{\text{ref}} / \text{M}$	$(175.43 \pm 0.14) \cdot 10^{-4}$	$(158.07 \pm 0.15) \cdot 10^{-4}$
C_B / M	$(41.82 \pm 0.11) \cdot 10^{-4}$	$(39.66 \pm 0.11) \cdot 10^{-4}$
$[\text{OH}]_{\text{ref}} / \text{M}$	$(26.63 \pm 0.12) \cdot 10^{-4}$	$(26.63 \pm 0.12) \cdot 10^{-4}$
$Q / \text{mol} \cdot \text{kg}^{-1}$	1.51 ± 0.04	$(31.90 \pm 0.93) \cdot 10^{-2}$
$S_e / \text{m} \cdot \text{g}^{-1}$	17.5 ± 1.8	$84.74 \pm 1.82 (\text{N}_2)$
Total number of coordination sites	$(36.4 \pm 5.4) \cdot 10^{18}$	$(21.96 \pm 0.68) \cdot 10^{18} (\text{Kr})$
Coordination sites density / nm^{-2}	52.0 ± 5.5	$(43.0 \pm 2.3) \cdot 10^{18} (\text{Kr})$
		$2.3 \pm 0.1 (\text{N}_2)$
		$875 \pm 37 (\text{Kr})$

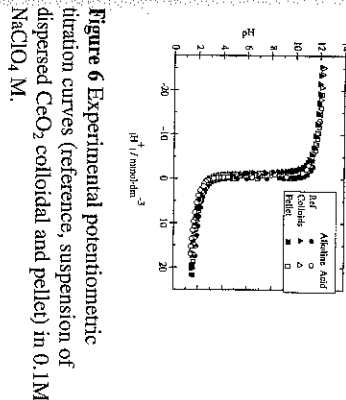


Figure 6 Experimental potentiometric titration curves (reference, suspension of dispersed CeO₂ colloidal and pellet) in 0.1M NaClO₄ M.

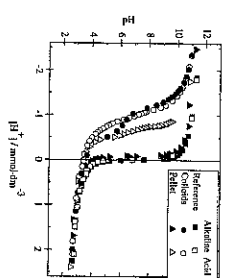


Figure 7 Zoom of the Figure 8 close to the zero charge point region.

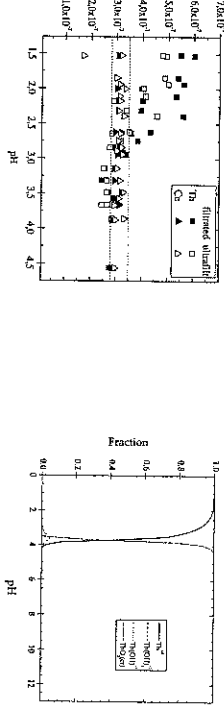


Figure 8 [Th] and [Ce] (filtered and ultrafiltered samples) in Th sorption experiments as a function of pH.

Figure 9 Aqueous Th(IV) speciation curves as a function of pH for ionic strength 0.1M and [Th] = $6 \cdot 10^{-5} \text{ M}$.

On one hand, the knowledge of surface sites density is essential because it is a controlling parameter in dissolution and precipitation processes and, on the other hand, surface complexation models require input this parameter, but no works related with CeO_2 pellet was found to compare our results. From these results is possible to conclude that ceria surface has certain tendency to retain protons on its surface. However, to refine the results, potentiometric titration at different ionic strengths should be made and use other techniques as well.

Because of Pu solubility is higher than Ce one in aqueous solutions, experiments with Pu should also be done to observe the effects on Th adsorption, as well as Th sorption essays at constant pH to get the distribution coefficient.

REFERENCES

1. K. D. Weaver and J. S. Herring, *Nuclear Technology* **143**, 22 (2003).
2. L. C. Walters, D. L. Porter and D. C. Crawford, *Progress in Nuclear Energy* **40**, 513 (2002).
3. R. P. C. Schram and F. C. Klaassen, *Progress in Nuclear Energy* **49**, 617 (2007).
4. C. Kuetayayali, *Report No. JRC-IU-TN-2007779*, 2007.
5. R. C. Ewing, *Progress in Nuclear Energy* **49**, 635 (2007).
6. G. R. Choppin, *Marine Chemistry* **99**, 83 (2006).
7. E. Östhols, PhD. Thesis, Royal Institute of Technology, Stockholm, Sweden, 1994
8. M. H. Bradbury and B. Baeyens, *Geochim. Cosmochim. Acta* **69**, 875-892 (2005).
9. E. Östhols, *Geochim. Cosmochim. Acta* **59**, 1235 (1995).
10. E. Iglesias and J. Quiñones, *App. Surf. Science* **254**, 6890 (2008)

ABSTRACT

Garnets, $\text{A}_3\text{B}_2\text{C}_3\text{O}_{12}$, are considered to be potential host phases for the immobilization of high-level nuclear waste as they can accommodate a number of elements of interest, including Zr, Ti and Fe. The naturally occurring garnet, kimzeyite, $\text{Ca}_3(\text{Zr}, \text{Ti})_2(\text{Si}, \text{Al}, \text{Fe})_3\text{O}_12$, can contain $\sim 30\text{wt\%}$ Zr. An understanding of the radiation tolerance of these materials is crucial to their potential use in nuclear waste immobilization. In this study two synthetic analogues of kimzeyite of composition $\text{Ca}_3\text{Zr}_2\text{FeAlSiO}_12$ and $\text{Ca}_3\text{Hf}_2\text{FeAlSiO}_12$ were monitored *in situ* during irradiation with 1.0 MeV Kr ions using the intermediate voltage electron microscope- Tandem User Facility (IVEM) at Argonne National Laboratory. The structure of these materials was previously determined by neutron diffraction and ^{57}Fe Mössbauer spectroscopy. $\text{Ca}_3\text{Zr}_2\text{FeAlSiO}_12$ and $\text{Ca}_3\text{Hf}_2\text{FeAlSiO}_12$ have very similar structural properties with cubic Ia3d symmetry, the only significant difference being the presence of Zr and Hf, respectively, on the 6 coordinated B sites.

INTRODUCTION

Naturally occurring garnets are found with a large range of elemental compositions with the cations located across more than one site in the lattice, e.g., schorlomite. Garnets can be prepared containing U, Th and Lanthanide elements; as such they make ideal candidates for the long-term storage of actinide waste. Current research in new materials for actinide waste tend to contain titanium and zirconium, this was originally due to the existence of compatible Ti phases for high-level waste, e.g., hollandite, pyrochlore and zirconolite. Zirconium has been added in recent research to enhance the stability to radiation damage. In nature there are two garnets that make ideal candidates for waste form research that have high levels of Ti^{4+} (schorlomite) or Zr^{4+} (kimzeyite), with kimzeyite and simplified analogues being the focus of this work. A schematic of the garnet structure is shown in Figure 1.

Kimzeyite $\text{Ca}_3(\text{Zr}, \text{Ti})_2(\text{Si}, \text{Al}, \text{Fe})_3\text{O}_12$ [1-5] was originally reported in 1961 for a sample from Magnet Cove in Arkansas, it is a naturally occurring garnet that contains high levels of Zr ($\sim 30\text{wt\%}$ ZrO_2). There have been two subsequent analyses published based on samples from the Aeolian Islands, and the Sabatini Volcanic district, both in Italy. All three analyses give similar values for elemental composition and crystal parameters. As these garnets are naturally occurring with good long-term stability, they are ideal to study as potential storage media for radioactive nuclear waste.

In this work we have irradiated $\text{Ca}_3\text{Zr}_2\text{FeAlSiO}_12$ and $\text{Ca}_3\text{Hf}_2\text{FeAlSiO}_12$, which have previously been studied to determine the cation location within the lattice using combined Mossbauer and neutron diffraction techniques. This work found that the Zr/Hf located on the B-site (in octahedral coordination with oxygen) with $\text{Fe}/\text{Al}/\text{Si}$ locating on the C-site (in tetrahedral coordination with oxygen). The results from the synthetic samples were then compared with electron channeling analysis of naturally occurring kimzeyite.

In Situ Radiation Damage Studies of $\text{Ca}_3\text{Zr}_2\text{FeAlSiO}_12$ and $\text{Ca}_3\text{Hf}_2\text{FeAlSiO}_12$

Karl R. Whittle¹, Mark G. Blackford¹, Gregory R. Lumpkin¹, Katherine L. Smith¹, and Nestor J. Zaluzec²

¹Institute of Materials Engineering, Australian Nuclear Science and Technology Organisation, PMB1, Menai, NSW 2234, Australia

²Argonne National Laboratory, 9700 South Cass Avenue, Argonne, IL 60439, USA